Comparison of Deconvolution Methods for the Structure Analysis of the Impact Areas on Jupiter

J. Babion (University Observatory, Munich, E-MAIL: babion@hal2.usm.uni-muenchen.de)
H. Boehnhardt (University Observatory, Munich),
F. Murtagh (ST-ECF ESO, Garching),
J.L. Starck (CEA, DSM/DAPNIA, CE-SACLAY, 91191 Gif-sur-Yvette Cedex)
U. Thiele, K. Birkle, T. Herbst (Max-Planck-Institute for Astronomy, Heidelberg),
D. Hamilton (Max-Planck-Institue for Nuclear Physics, Heidelberg),
J. L. Ortiz (Instituto de Astrofisica de Andalucia, Granada)

February 23, 1995

Abstract

Different deconvolution methods, the van Cittert method, the Lucy algorithm and a wavelet transform technique, are applied to visual and IR images of the SL9 impact areas on Jupiter.

The visual CCD images were obtained at the 1.2 m telescope and the IR frames at the 3.5 m telescope of the Calar Alto Observatory in Spain from 16-22 July 1994.

Because of short image exposure times, stars inside the frames are usually not available for the construction of a suitable point spread function (PSF). We examine the possibility of modelling a PSF based upon the essentially non-stellar images of Galilean satellites present in the frames and determine the influence of these artificial PSFs on the deconvolution results. We also vary different parameters of the algorithms to investigate their effects on the sharpening of the surface structures on Jupiter.

1 Observations and Data Reduction

The visual and IR images used in our analysis were taken at Calar Alto Observatory in Spain during 16-22 July 1994. In each night Jupiter was observed from about 19:15 to 22:30 UT.

Table 1 summarizes the information on the instruments and data reduction procedures as far as they are relevant for this work. For the visual wavelength range the typical exposure time was 1 second. In the IR we considered Jupiter images both from individual read-outs of typical 0.1 sec integration time as well as integrated frames which contain the average of several 10 individual read-outs. In the visual frames the Galilean moons are always imaged simultaneously with Jupiter, but only occasionally in the IR because of the much smaller field of view.

2 Image Deconvolution: Richardson-Lucy, Wavelet, van Cittert

An image is defined by its intensity distribution $I(x, y)$, corresponding to a "real image" $O(x, y)$ which is observed through the atmosphere and an optical system. If the imaging

wavelength	telescope	CCD	jupiter size (pixel)	pixel resolution	data reduction
visual	1.2 m	1024x1024	76	0.51"	bias, flatfield,
infrared	3.6 m	256x256	117	0.33"	bias, flatfield, bad pixels, sky subtraction

Table 1: Telescope and image data, data reduction processes

system is linear and shift-invariant, the relation between the object and the image in the same coordinate frame is a convolution:

$$I(x,y) = (O * P)(x,y) + N(x,y) \tag{1}$$

$P(x,y)$ is the point spread function (PSF) of the imaging system including atmosphere, and $N(x,y)$ is an additive noise term.

In Fourier space equation (1) leads to

$$\hat{I}(u,v) = \hat{O}(u,v)\hat{P}(u,v) + \hat{N}(u,v) \tag{2}$$

where symbol $\hat{}$ denotes the Fourier transform. We know $I(x,y)$ and we estimate $P(x,y)$. From this we want to determine $O(x,y)$. Problems occur from the cut-off frequency of the PSF and the existence of noise in the data. Furthermore, also discretisation and the lack of an appropriate PSF in the images causes problems in our application to Jupiter. For equation (2) there is no unique least-square solution of minimum norm $\|I(x,y) - P(x,y) * O(x,y)\|^2$.

The Richardson-Lucy (RL) method [2] uses an iterative approach for computing the maximum likelihood. As an enhancement to the RL method effective noise suppresion can be incorporated into the iteration by feeding back only significant structures of the residual. These structures are obtained by wavelet transform [3]. A similar modification can be made to other iterative algorithms such as that of van Cittert [1].

3 Application to Jupiter Images

In the following we describe our experience in applying all three deconvolution methods mentioned above to visual and IR images of Jupiter obtained during the SL9 impact period.

3.1 Visual Images

For the visual CCD frames we applied the Richardson Lucy algorithm with 100 iterations.

Fig. 1-4 show a visual frame of Jupiter taken on 22 July 1994, 20:22 UT, through Johnson B filter and the results of the applied deconvolution methods. The dark spots in the upper (southern) part of the Jupiter disk are the K(8), W(1) and U(2) impact sites (revolution cycle in paranthesis). The tiny dot on the right side is Europa just before occultation.

In Fig. 2 can cleary be seen, that the van Cittert method is not useful in our case. Good results are achieved by simple RL and RL with noise suppression (for instance two white spots can be clearly identified, which are only marginally seen in the original frame). The noise suppression enhancement has little effect, since the signal-to-noise ratio (SNR) is high in the visual frames.

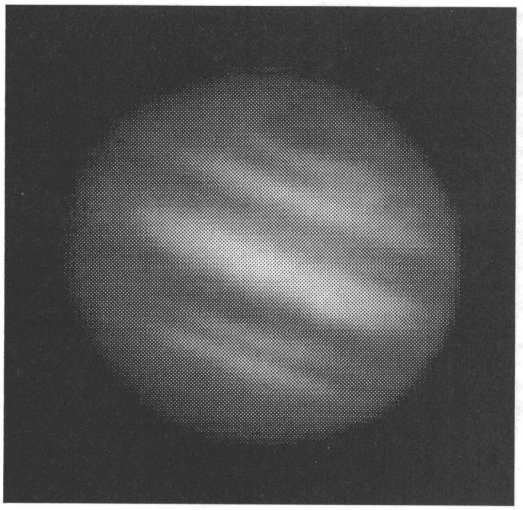

Figure 1: Original Image

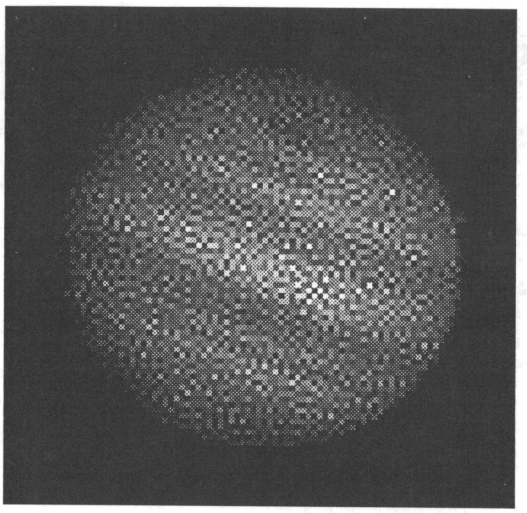

Figure 2: van Cittert Deconvolution

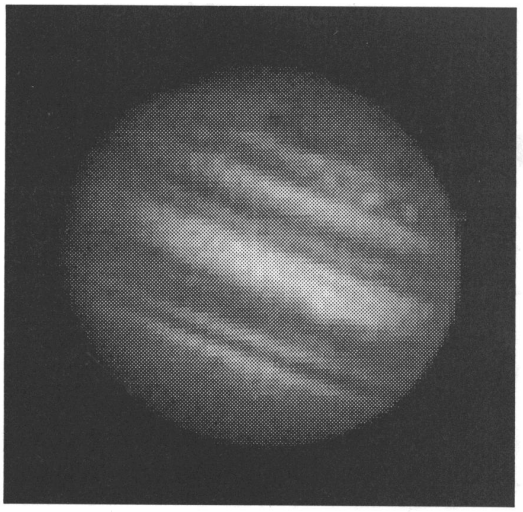

Figure 3: Richardson-Lucy

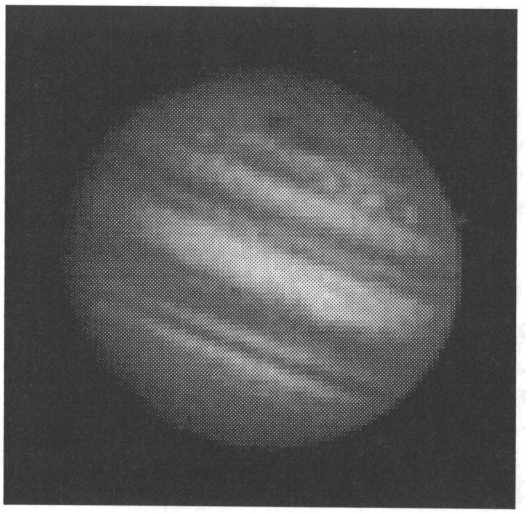

Figure 4: Richardson Lucy with wavelet noise suppression

3.2 Infrared Images

The infrared frames were also processed with the Richardson Lucy algorithm in 100 iterations.

Fig. 5 shows the original image of Jupiter, observed at 21 July 1994, 19:17 UT, through 1.7 μm methane filter. The Great Red Spot is clearly visible, the impact sites are from bottom to top: E-F-T-complex, H, Q1, G-D-S-R-Q2-complex and L on the limb. In Fig. 6-8 the results of the different deconvolution methods are shown.

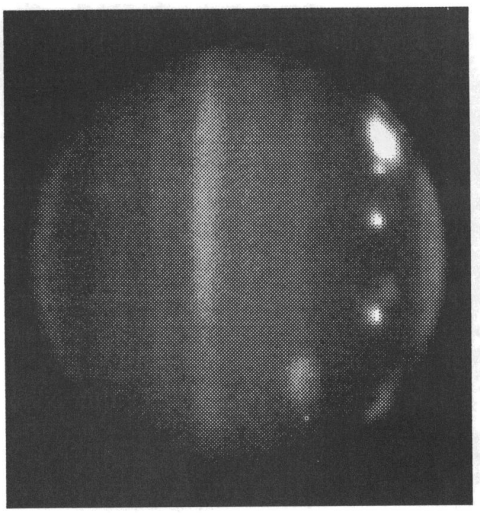

Figure 5: Original Image

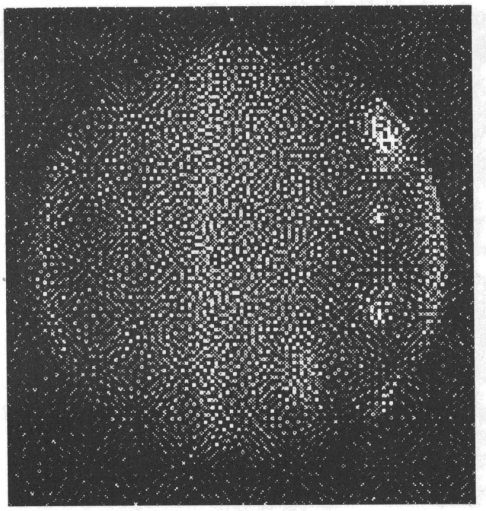

Figure 6: van Cittert Deconvolution

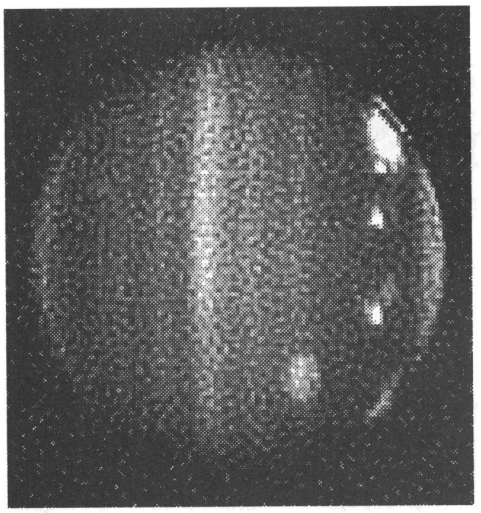

Figure 7: Richardson-Lucy

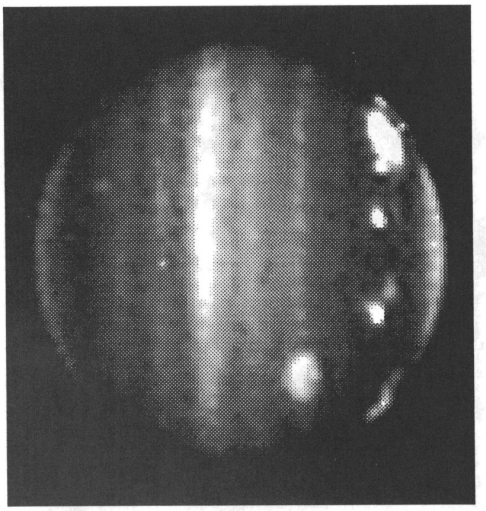

Figure 8: Richardson-Lucy with multiresolution

Similar to the visual images, the van Cittert method is not useful for IR frames. Simple RL yields to noisy artefacts instead of increasing sharpness. Only for RL plus wavelet noise-suppression the artefacts disappear, and more detailed structures than in the original data can be seen.

3.3 Point Spread Function

The structure of the PSF is very much determined by the time variable atmospheric seeing. Usually one may use a star in the frame as reference to examine the individual PSF for the exposure. For our Jupiter images this approach is not possible, because the exposure times were too short to show stars in the frames.

As an alternative approach, a set of Gaussian point spread functions with full width at half maximum (FWHM) from 0.1 to 5 pixels was used, which covers the most likely FWHM for the

exposures of about 2 pixels. The effects of badly chosen FWHM PSFs on RL deconvolution can be seen for the visual range in Fig. 9 and Fig. 10 and for IR in Fig. 11 and Fig. 12.

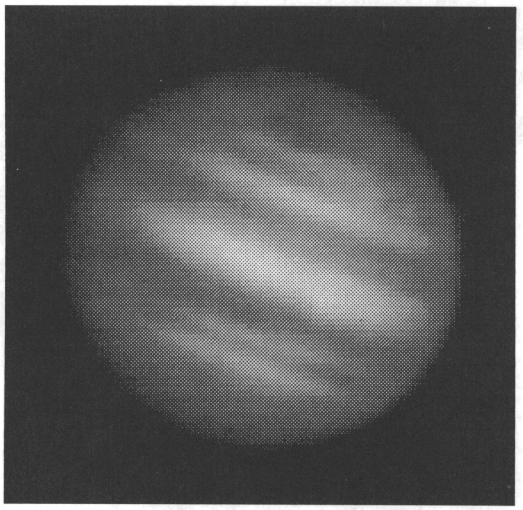

Figure 9: The visual image of Fig. 1, deconvolved with PSF of 0.1 pixel FWHM

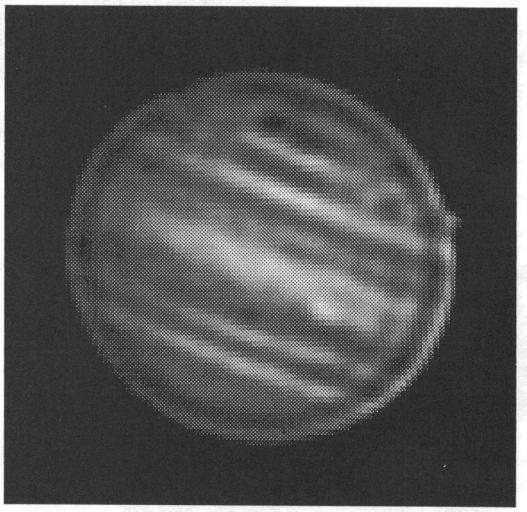

Figure 10: The same visual image, deconvolved with PSF of 5.0 pixel FWHM

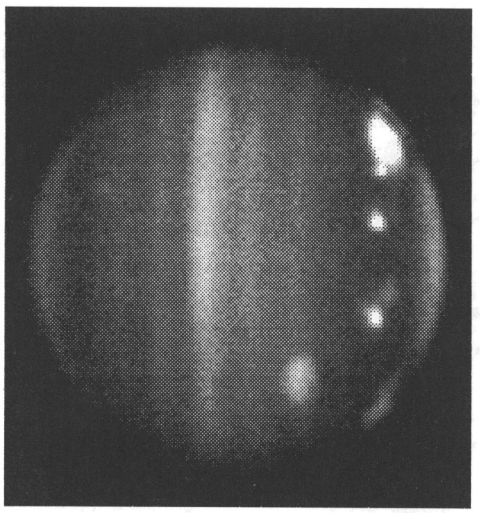

Figure 11: IR image of Fig. 5, deconvolved with PSF of 0.2 pixel FWHM

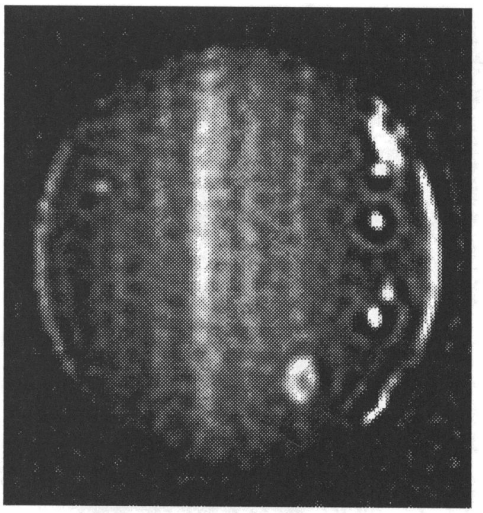

Figure 12: the same IR image, deconvolved with PSF of 5.0 pixel FWHM

Too narrow PSFs cause blurring of surface structures, while too wide PSFs produce dark rings around regions of large contrast.

In the future we will examine the possibility of modelling the actual PSF based upon the essentially non-stellar images of Galilean satellites present in the frames. The idea is the following: modelling the satellite as disk, then deconvolve the images of the moons with the constructed disk to get the PSF.

3.4 Number of RL Iterations

The number of iterations affects the quality of the results. For our Jupiter images typically of the order of 100 iterations are required. More iterations do not lead to a further improvement.

3.5 Number of Wavelet Scales

Fig. 13 shows the wavelet transforms calculated for the visual Jupiter image of Fig. 1 at scales 1 to 4. Evidently, wavelet transforms up to scale 4 are sufficient for noise suppression in RL deconvolution of our Jupiter images. Structural information is no longer present in wavelet scales of 4 and higher.

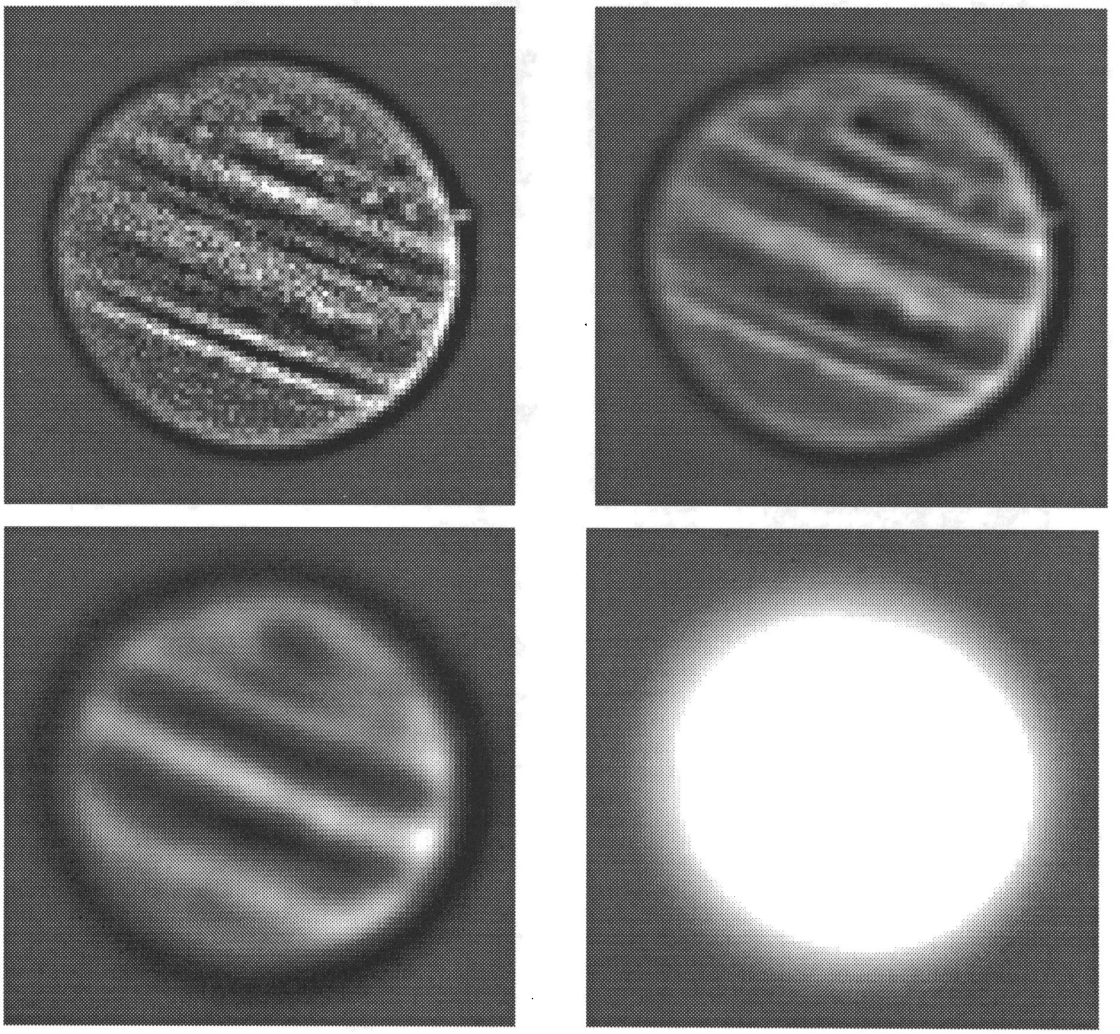

Figure 13: Scales 1 to 4 of the wavelet transform of the Jupiter image of Fig.1

References

[1] van Cittert, P.H.: 1931, Z.Physik 69, 298
[2] Lucy, L.B.: 1974, AJ 79,745
[3] Starck J.L., Murtagh F.: 1994, A&A 288, 342